

ARTEMIS observations of lunar pick-up ions in the terrestrial magnetotail lobes

A. R. Poppe,^{1,2} R. Samad,¹ J. S. Halekas,^{1,2} M. Sarantos,^{2,3,4} G. T. Delory,^{1,2} W. M. Farrell,^{2,4} V. Angelopoulos,⁵ and J. P. McFadden¹

Received 27 June 2012; revised 3 August 2012; accepted 6 August 2012; published 15 September 2012.

[1] We report observations by the twin-probe mission ARTEMIS of pick-up ions of lunar origin obtained during times when the Moon was within the terrestrial magnetotail lobes. These ions were detected as two separate focused beams above the dayside lunar surface. Analysis of these beams has shown that they possess both field-aligned and field-perpendicular velocities, implying the presence of electric fields both parallel and perpendicular to the magnetotail lobe magnetic field. We suggest that the sources of these two electric fields are (a) the near-surface electric field due to the lunar photoelectron sheath and (b) the electric field generated by the magnetotail lobe convection velocity. We use the energy and pitch angle spectra to constrain the source locations and compositions of these ions, and conclude that exospheric ionization of the neutral exosphere is the dominant lunar pick-up ion production mechanism in the tail lobes. **Citation:** Poppe, A. R., R. Samad, J. S. Halekas, M. Sarantos, G. T. Delory, W. M. Farrell, V. Angelopoulos, and J. P. McFadden (2012), ARTEMIS observations of lunar pick-up ions in the terrestrial magnetotail lobes, *Geophys. Res. Lett.*, 39, L17104, doi:10.1029/2012GL052909.

1. Introduction

[2] The Moon does not possess a significant atmosphere, but is known to have a tenuous surface-bounded exosphere consisting of a collection of neutral species originating either from inside or on the surface of the Moon [Stern, 1999]. These exospheres, technically multiple since they are collisionless and thus do not interact with one another, are generated via a variety of processes including thermal desorption, photon-stimulated desorption, sputtering by high-energy ambient plasma, and micrometeoroid bombardment. The lunar exosphere has been studied by ground-based observation of neutral resonance lines [Mendillo et al., 1993; Potter et al., 2000; Wilson et al., 2006], in-situ mass spectrometry [Hoffman et al., 1973], and observation of freshly-ionized

exospheric constituents as pick-up ions [Hilchenbach et al., 1993; Mall et al., 1998; Yokota et al., 2009; Halekas et al., 2012]. Despite these observations, a complete understanding of the lunar exosphere is not yet in hand.

[3] At the Moon, pick-up ions are generated via photoionization of lunar exospheric neutrals, photon- and electron-stimulated desorption of surface constituents, and impact ionization from energetic plasma and incident micrometeoroid bombardment [Stern, 1999; Hartle and Killen, 2006]. Most lunar pick-up ion observations to date have occurred in the solar wind, where the combination of the large solar wind convection speed and magnetic field give rise to convection electric fields on the order of tens of millivolts per meter; however, freshly-born ions should be picked-up any time a convecting magnetic field is present. As the Moon orbits the Earth, it passes through the terrestrial magnetotail for approximately five days out of every month. During this time, the Moon is exposed to a variety of ambient plasma environments, including the magnetosheath, the plasma sheet, and the tail lobes. In the magnetosheath and plasma sheet, ambient plasmas typically dominate the near-Moon plasma environment; however, the near vacuum of the tail lobes presents an opportunity to study plasma originating from the Moon itself. Ions originating from the Moon have been previously measured in the magnetotail lobe by the KAGUYA spacecraft, and identified as a combination of He⁺, C⁺, O⁺, Na⁺, K⁺, and Ar⁺ ions [Tanaka et al., 2009], although, Al⁺ and Si⁺ could also contribute to the measured spectra [Saito et al., 2010].

[4] In this paper, we present two observations by the Acceleration, Reconnection, Turbulence, and Electrodynamics of the Moon's Interaction with the Sun (ARTEMIS) spacecraft, currently in orbit around the Moon [Angelopoulos, 2010], of ions originating above the lunar dayside while in the terrestrial magnetotail lobes. Section 2 presents and discusses the ARTEMIS observations, while Section 3 analyzes the results to determine the source and composition of the pick-up ions. Finally, we conclude and outline future work in Section 4.

2. ARTEMIS Observations

[5] The ARTEMIS mission consists of two probes with comprehensive plasma and fields instrumentation in elliptical orbits around the Moon [Angelopoulos, 2010]. We present measurements made by the ARTEMIS P2 spacecraft on October 13, 2011 and November 11, 2011, using the low energy electron and ion Electrostatic Analyzer (ESA) [McFadden et al., 2008] and the Fluxgate Magnetometer (FGM) [Auster et al., 2008]. During these observations, the Moon was in the terrestrial magnetotail lobe at GSE positions of [−60.9, −16.7, 3.66] R_E and [−62.5, −7.5, 2.0] R_E ,

¹Space Sciences Laboratory, University of California, Berkeley, California, USA.

²NASA Lunar Science Institute, Ames Research Center, Mountain View, California, USA.

³Goddard Planetary Heliophysics Institute, University of Maryland, Baltimore County, Baltimore, Maryland, USA.

⁴NASA Goddard Space Flight Center, Greenbelt, Maryland, USA.

⁵Department of Earth and Space Sciences and Institute of Geophysics and Planetary Physics, University of California, Los Angeles, California, USA.

Corresponding author: A. R. Poppe, Space Sciences Laboratory, University of California, 7 Gauss Way, Berkeley, CA 94720, USA. (poppe@ssl.berkeley.edu)

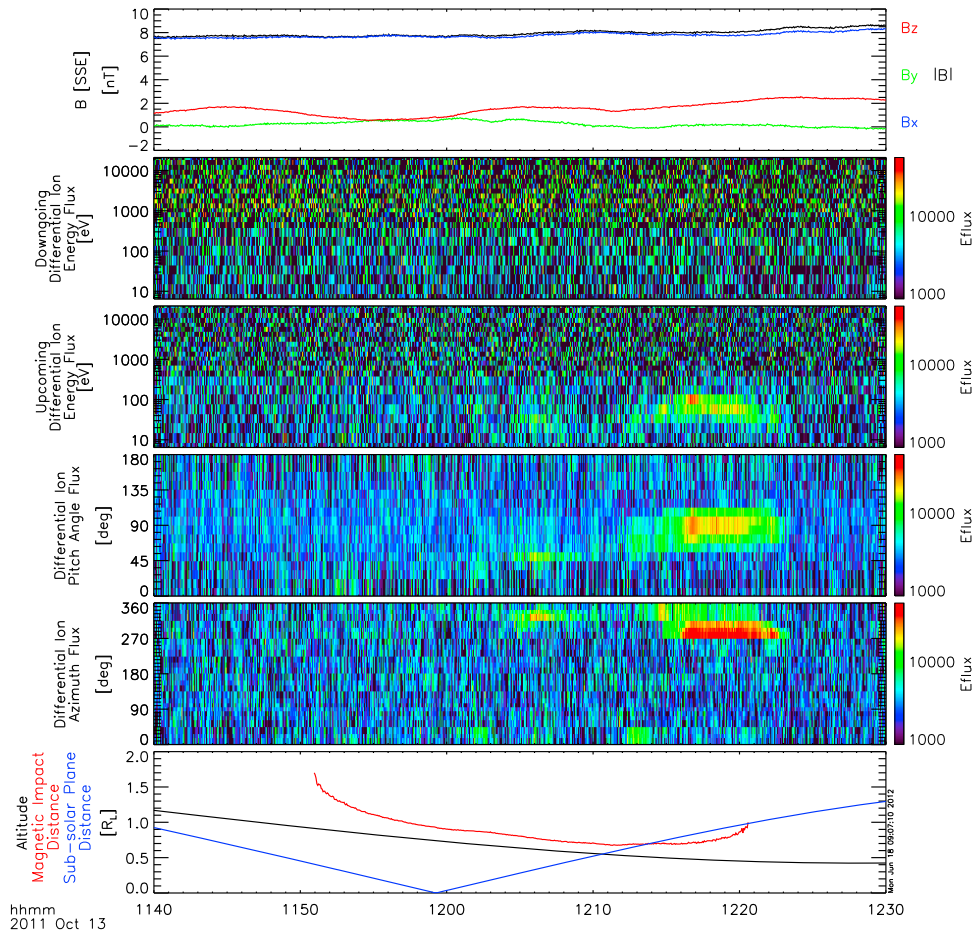


Figure 1. A time-series of ARTEMIS P2 measurements on October 13, 2011, in the terrestrial magnetotail lobe, as explained in the text. Energy flux is measured in units of $\text{eV}/\text{cm}^2/\text{s}/\text{str}/\text{eV}$.

respectively. For both dates, the P2 orbits were such that the spacecraft was within one lunar radius of the dayside lunar surface. Additionally, on both October 13 and November 11, the geomagnetic K_p index was 1-, indicating calm geomagnetic conditions. Figures 1 and 2 show the ARTEMIS observations from October 13 and November 11, 2011, respectively, in identical formats. In the top panel, the magnetic field magnitude (black) and components (colors) are displayed, showing a dominant, positive B_x component in both observations, typical of the terrestrial magnetotail north lobe. The second through fifth panels show the downgoing (tailward) energy, upcoming (earthward) energy, pitch angle, and azimuth ion spectra, respectively. The azimuthal angle is defined in the spacecraft spin plane (very close to the ecliptic plane), with 0° along the Sun-Moon vector. The bottom panel shows the spacecraft altitude (black), magnetic connection distance, defined as the distance between the ARTEMIS spacecraft and the lunar surface along the instantaneous magnetic field line (red), and the lateral (Y SSE) distance from the lunar noon-midnight meridional plane (blue).

[6] On both dates, ARTEMIS observed no significant ion flux in the downgoing (tailward) direction and a pair of ion beams in the upcoming (earthward) direction, one of short duration and one of long duration above the dayside lunar

surface, respectively. In the October observation, the beams are seen at 12:05–12:08 and 12:13–12:22 UTC, respectively, while in the November observation, the beams are at 10:53–10:55 and 11:02–11:17, respectively. The ion beams are between roughly 20 and 175 eV, with the ions during the November observation at slightly higher energies. For the long-duration beams, the October observation shows a mostly constant energy centered at approximately 100 eV, while the November observation shows a dispersion in energy starting at approximately 175 eV and falling to 20 eV by the end. In both observations, the ARTEMIS spacecraft potential was roughly constant at approximately +40 V, indicating maximum net ion energies of 140 eV and 215 eV, respectively, for the October and November observations. In the pitch angle spectra, the October and November short-period beams appear at approximately 45° and 30° , respectively. In contrast, the long-period beam of ions in October is concentrated almost entirely at 90° , with a slight excursion to smaller pitch angles at the beginning of the observation. In November, the pitch angle spectrum for the long-period ions has a dispersion signature from approximately 30° to 90° correlated with the dispersion in energy. In the azimuth spectra, all four beams are clearly and narrowly beamed, often appearing within a single angular bin. Finally, while the

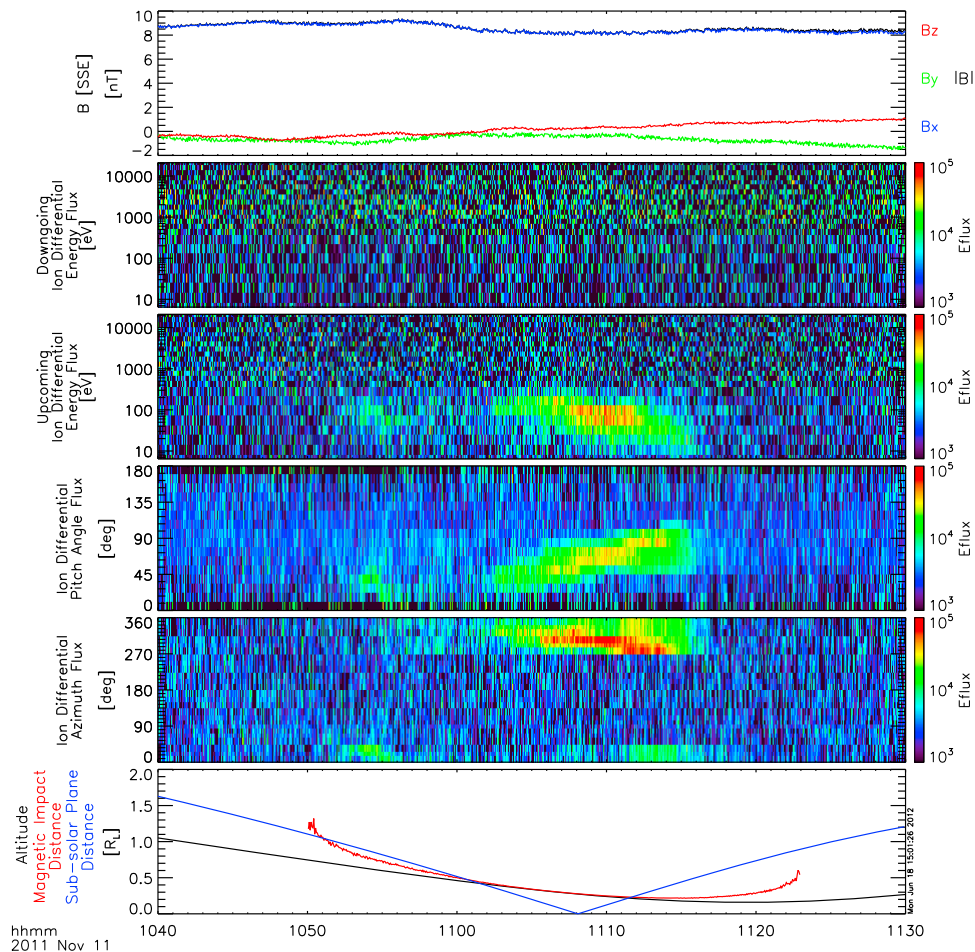


Figure 2. A time-series of ARTEMIS P2 ion measurements on November 11, 2011 in the terrestrial magnetotail lobe, as explained in the text. Energy flux is measured in units of $\text{eV}/\text{cm}^2/\text{s}/\text{str}/\text{eV}$.

short- and long-period beams are separated by approximately the same distance in both observations, the October beams are displaced in the +Y SSE direction almost $1.5 R_L$ relative to the November observations.

3. Analysis

3.1. Source Region Constraints

[7] In order to understand and constrain the composition, source regions, and source processes of these ions, we must analyze the ion behavior in both energy and pitch angle during each observation. To guide this analysis, Figure 3 shows a cartoon representation of the fields and particle populations relevant for these ARTEMIS observations. The Moon (gray) is embedded in the magnetotail lobe magnetic field (black), which is highly coherent and dominantly in the $\pm X$ SSE direction, with potentially slight components in the Y or Z SSE directions. The terrestrial magnetotail lobe fields are known to convect, and in the lunar frame, this convection produces an electric field, \mathbf{E}_c , on the order of tenths of millivolts (roughly one to two orders of magnitude smaller than in the solar wind) [Troshichev *et al.*, 1999]. Any newly-born ion will gyrate around the magnetic field, \mathbf{B} , while its gyro-center drifts with a characteristic velocity, $\mathbf{v}_c = \mathbf{E}_c \times \mathbf{B}/B^2$, equal to the magnetotail convection velocity (red). A second electric field is produced near the lunar surface via

the photoemission of electrons from the lunar surface due to incident solar ultraviolet radiation (orange). As photoelectrons are emitted from the lunar surface, they generate an electric field (blue) between the positively-charged lunar surface and the cloud of emitted photoelectrons. The best constraint on the strength of both the photoelectric field and electric potential at the surface of the Moon in the tail lobes comes from the Apollo 14 Charged Particle Lunar Environment Experiment (CPLEE), which inferred a lunar surface potential in the range of +40–200 V, with corresponding electric field strengths of ≈ 5 V/m extending approximately 25–250 m above the lunar surface (although, this thickness is not well constrained in the tail lobes) [Reasoner and Burke, 1972].

[8] Also depicted are nominal trajectories for two ions with different source locations. For ions born close to the surface (green), within the photoelectron sheath, the ion will experience a combination of parallel and perpendicular acceleration. To a good approximation near the sub-solar point, the photoelectron sheath field will accelerate ions mainly parallel to the magnetic field in a short distance above the lunar surface, while the convection electric field (along with the lobe magnetic field) will cause the ion to simultaneously gyrate about the lobe magnetic field and drift with the lobe convection velocity. In sum, the photoelectric field and the convection electric field will cause the ion to drift earthwards and with the

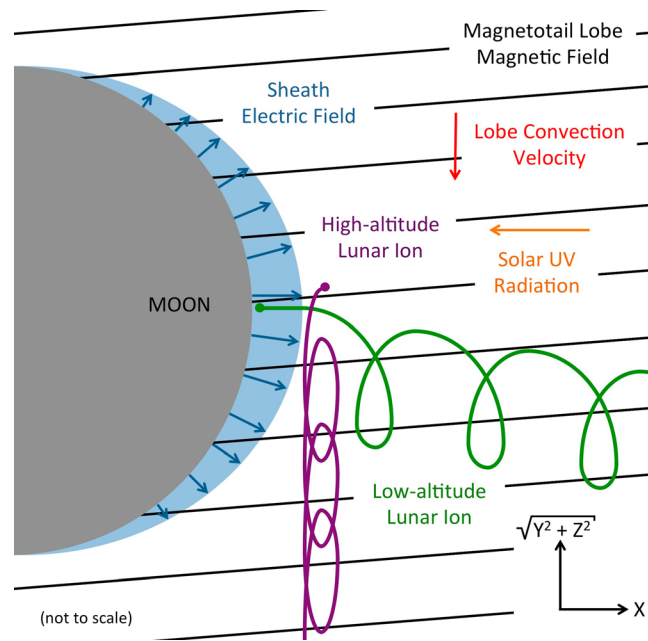


Figure 3. A cartoon depicting the geometry and fields present during the ARTEMIS observations as described in the text.

lobe magnetic field. For ions born high above the lunar surface relative to the photoelectron sheath thickness (purple), the photoelectric field is weak and/or non-existent and thus, the ion is only accelerated by the magnetotail lobe convection electric field, completely perpendicular to the magnetic field. These two end-member scenarios will result in ions with distinctly different pitch angle spectra: the low-altitude ions (green) will have pitch angles less than 90° due to their combination of parallel and perpendicular velocities from the sheath and convection electric fields, while the high-altitude ions (purple) will have strictly 90° pitch angles since they start with zero velocity and drift perpendicular to the field.

[9] In the two ARTEMIS observations presented, the long-period ions have a range of pitch angles, with a brief period of ions between 60° and 90° followed by an extended period of 90° during the October observations and pitch angles from 30° to 90° in the November observation. This requires an extended photoionization source region, as ions must be produced in regions both within and outside of the lunar photoelectron sheath in order to have a range of parallel velocities and in turn, pitch angles. Furthermore, in the November observation, these ions have a clear correlation between pitch angle and energy, with the low-pitch angle ions appearing with the highest energy, corresponding to their acceleration and focusing from the photoelectric field. Given these facts, the source of the long-period ions must be photoionization of the lunar neutral exosphere. In contrast, the short-period ions appear on both days with relatively narrow pitch angle distributions between roughly 30° and 45° . Therefore, these ions must be produced entirely within the photoelectron sheath, either directly from or near the lunar surface. Given that typical neutral exosphere scale heights are many times the expected photoelectron sheath thickness [Hartle and Killen, 2006], the narrow pitch angle distribution of the short-period ions further implies a source directly from the lunar surface, since exospheric photoionization would produce a much broader range of pitch angles. Production mechanisms operating in the tail lobe that generate ions

directly from the surface include micrometeoroid bombardment, and photon- and electron-stimulated desorption; however, all of these mechanisms would be expected to operate across the entire surface of the Moon, rather than only at a discrete location as observed. One possibility for the presence of ions with such narrow pitch angle and energy spectra may be the photo-ionized products of neutrals vented from a localized source in the lunar crust, similar to local sources found by alpha particle measurements of the radioactive decay of lunar ^{222}Rn and its subsequent daughter products [Bjorkholm et al., 1973; Lawson et al., 2005]. The most recent ^{222}Rn observations from Lunar Prospector were mainly found on the lunar near-side at the Aristarchus and Kepler craters, which are on the lunar dayside during the ARTEMIS observations presented here.

3.2. Ion Composition Constraints

[10] As a pick-up ion gyrates about the magnetic field, it will obtain a maximum perpendicular energy of $E_{\text{max}} = 2m_i v_c^2$, where m_i is the ion mass [Hartle and Killen, 2006]. Figure 4 shows a contour plot of the maximum perpendicular pick-up ion energy as a function of ion mass and convection speed. Also marked in purple are several candidate ion species that are most likely to constitute the ion populations observed by ARTEMIS given previous observations of pick-up ions in the tail lobes and recent modeling of the neutral exosphere [Tanaka et al., 2009; Saito et al., 2010; Sarantos et al., 2012]. We can compare these masses to the maximum perpendicular ion energy observed by ARTEMIS for the long-period ions during both the October and November events. In the October event, a majority of the long-period ions appear at 90° pitch angle, and thus, the maximum observed energy of approximately 100 eV is completely perpendicular. Adding in the spacecraft potential, approximately +40 V, yields a maximum ion energy of 140 eV. For the November event, the pitch angle varies from approximately 30° to 90° , as the relative amounts of parallel and perpendicular velocity change. After adding in the spacecraft potential of approximately

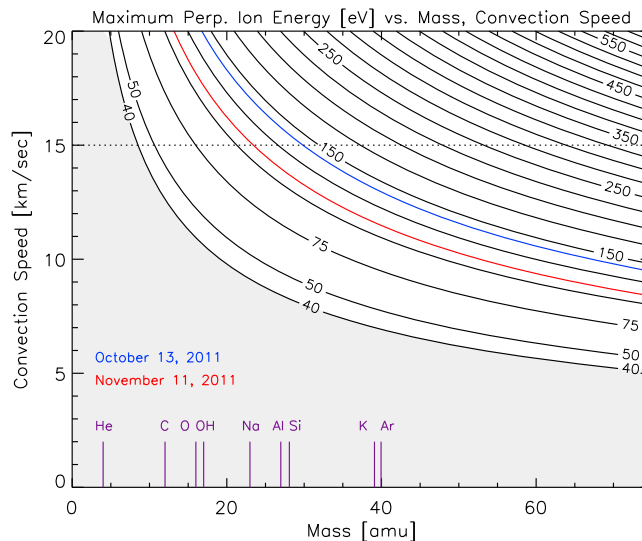


Figure 4. A contour plot of the maximum perpendicular energy obtainable by a pick-up ion as a function of ion mass and convection velocity. Overplotted as blue and red contour lines are the maximum observed perpendicular ion energies from the October 13, 2011 (140 eV) and November 11, 2011 (110 eV) observations, respectively. The dotted line denotes the typical magnetotail lobe convection speed expected for these two dates. Additionally, the masses of several candidate species are marked in purple. The grey shaded region denotes combinations of masses and convection speeds that ARTEMIS cannot measure due to a typical spacecraft potential in the tail lobes of approximately +40 V.

+40 V, the maximum perpendicular energy occurs at a pitch angle of 60° at 110 eV.

[11] Both the October and November maximum perpendicular ion energies are over plotted on Figure 4 as blue and red contour lines, respectively. While ARTEMIS cannot directly measure the convection speed, *Troshichev et al.* [1999] have shown that for $Kp < 1+$, the average convection velocities at approximately $80\text{--}200 R_E$ in the north tail lobe at B_x values of approximately 8–10 nT have average values of $[v_x, v_y, v_z] = [-130, 7.5, -12.5] \text{ km s}^{-1}$. Taking the component of this velocity perpendicular to the lobe magnetic field yields a convection speed of approximately 15 km s^{-1} , denoted on Figure 4 with a dotted line. The mass at which this dotted line intersects the mass-convection speed contours from the October and November observations provides a lower limit to the possible ion mass, as we do not necessarily know that ARTEMIS measured the ions at the top of their cycloid. These limits for the October and November observations correspond to 29 and 24 amu, respectively, although, we caution that these values are approximate, given that we do not directly measure the convection speed.

[12] Nevertheless, these lower limits do allow us to make some interesting conclusions regarding the ion composition. We can rule out He^+ as a possible constituent given that it cannot attain enough energy to overcome the spacecraft potential barrier for reasonable convection speeds. C^+ , O^+ and OH^+ are unlikely to be constituents, although we cannot definitively rule them out given their close proximity to the lower mass limit and the uncertainty in the actual convection speed during each observation. This leaves Na^+ , Al^+ , Si^+ , K^+ , and Ar^+ as the most likely constituents for the long-period beam.

[13] Indeed, given the relatively short distance between the lunar surface and ARTEMIS relative to typical gyroradii for these species, it is possible that the long-period ion beam is composed of most, if not all, of these species, since the ions

will not have had sufficient distance to disperse according to their individual gyroradii. The short-period ions have perpendicular energies of approximately 65 and 90 eV, respectively, somewhat less than the long-period ions. In turn, the minimum mass constraint for these ions is somewhat lower than in the long-period ion case, implying a minimum mass of approximately 15 amu.

4. Conclusion

[14] We have presented two ARTEMIS observations of lunar-based ions while in the terrestrial magnetotail lobes. These ion populations appear on the lunar dayside, and have a combination of both parallel and perpendicular velocities. From this, we have inferred that freshly-ionized atoms from the lunar surface or exosphere in the tail lobes will experience a combination of two electric fields: (1) the near-surface photoelectric field which can accelerate ions both along and perpendicular to the magnetic field lines, and (2) the electric field produced by the convection of the terrestrial tail lobe magnetic fields, which can provide only perpendicular acceleration. This discovery is in contrast to previous reported observations of lunar-based ions in the terrestrial magnetotail lobes, which concluded that magnetotail lobe convection was too weak to accelerate ions to energies in the hundreds of eV and that photoelectric fields must be solely responsible [Tanaka et al., 2009]. We note that the observation of ion pick-up via magnetotail lobe convection implies that the behavior of lunar ions is dependent on the dynamics of the terrestrial magnetotail. In turn, pick-up ion dynamics in the tail are thus dependent on geomagnetic activity levels, as the correlation between tail lobe convection and geomagnetic activity is well-established [Troshichev et al., 1999]. Indeed, ARTEMIS has preliminary observations of these pick-up ions accelerated to energies up to 1 keV in the magnetotail on a moderately

disturbed day ($Kp = 2+$). Future work will statistically analyze the relationship between perpendicular pick-up ion energy and geomagnetic activity levels in order to further confirm this finding. Additionally, a measurement of the magnetotail convection velocity during an individual observation would help to constrain both the dynamics and the composition of these ions and we have begun preliminary work on using the method of lunar shadowing to determine tail lobe convection velocities at $60 R_E$ [McCoy et al., 1975].

[15] Analysis of the pitch angle spectra has allowed us to conclude that the long-period ions are produced by photoionization of a broad, extended neutral exosphere above the lunar dayside, while the short-period ions are ionized either directly from or very near the surface in a very narrow spatial region, possibly from a discrete geological vent. The flux of the long-period exospheric pick-up ions dominates the overall ion measurements in these observations, implying that in the tail lobes ionization of the neutral exosphere is a greater source of pick-up ions than either micrometeoroid bombardment, or electron- or photon-stimulated desorption. This compares favorably with recent estimates of pick-up ion fluxes in the solar wind, which concluded that even in the presence of solar wind sputtering (which is not present in the tail lobes), exospheric ionization is the dominant production mechanism for most lunar pick-up ion species [Sarantos et al., 2012]. An exception to this may be the effect of short, yet intense, micrometeoroid bombardment of the lunar surface when the Earth passes through a meteoroid stream, which is known to enhance the neutral exosphere but should also generate ions directly from the surface upon impact [Hunten et al., 1998; Smith et al., 1999]. Future ARTEMIS measurements of pickup ions in the tail lobes should be carefully analyzed for deviations in pitch angle and energy spectra from the measurements presented here and correlated with known meteor streams. Additionally, the observed ion energy flux may help to further constrain both the pickup ion production rate and associated neutral densities, although, a modeling approach is most likely required given the effect of the complicated electrostatic environment near the lunar surface on the pickup ion trajectories. Finally, while we have established minimum mass limits for the composition of these ions, simultaneous comparisons with upcoming in-situ observations of the neutral exosphere by the Lunar Atmosphere and Dust Environment Explorer will help to definitively identify the ion composition. Such comparisons may also yield additional information and constraints on the source regions, loss processes, and dynamics of the lunar neutral exosphere and its pick-up ion progeny.

[16] **Acknowledgments.** The authors gratefully acknowledge support from NASA's Lunar Science Institute. The ARTEMIS mission is funded and operated under NASA grant NAS5-02099. The Kp indices were downloaded from the NOAA NGDC database.

[17] The Editor thanks three anonymous reviewers for their assistance in evaluating this paper.

References

- Angelopoulos, V. (2010), The ARTEMIS mission, *Space Sci. Rev.*, *165*, 3–25.
- Auster, H. U., et al. (2008), The THEMIS fluxgate magnetometer, *Space Sci. Rev.*, *141*, 185–211.
- Bjorkholm, P. J., L. Golub, and P. Gorenstein (1973), Distribution of ^{222}Rn and ^{210}Po on the lunar surface as observed by the alpha particle spectrometer, *Proc. Lunar Sci. Conf.*, *4th*, 2793–2802.
- Halekas, J. S., A. R. Poppe, G. T. Delory, M. Sarantos, W. M. Farrell, V. Angelopoulos, and J. P. McFadden (2012), Lunar pickup ions observed by ARTEMIS: Spatial and temporal distribution and constraints on species and source locations, *J. Geophys. Res.*, *117*, E06006, doi:10.1029/2012JE004107.
- Hartle, R. E., and R. Killen (2006), Measuring pickup ions to characterize the surfaces and exospheres of planetary bodies: Applications to the Moon, *Geophys. Res. Lett.*, *33*, L05201, doi:10.1029/2005GL024520.
- Hilchenbach, M., et al. (1993), Observations of energetic lunar pick-up ions near Earth, *Adv. Space Res.*, *13*(10), 321–324.
- Hoffman, J. H., et al. (1973), Lunar atmospheric composition results from Apollo 17, *Proc. Lunar Sci. Conf.*, *4th*, 2865–2875.
- Hunten, D. M., et al. (1998), The Leonid meteor shower and the lunar sodium atmosphere, *Icarus*, *136*, 298–303.
- Lawson, S. L., W. C. Feldman, D. J. Lawrence, K. R. Moore, R. C. Elphic, R. D. Belian, and S. Maurice (2005), Recent outgassing from the lunar surface: The Lunar Prospector Alpha Particle Spectrometer, *J. Geophys. Res.*, *110*, E09009, doi:10.1029/2005JE002433.
- Mall, U., E. Kirsch, K. Cierpka, B. Wilken, A. Söding, F. Neubauer, G. Gloeckler, and A. Galvin (1998), Direct observation of lunar pick-up ions near the Moon, *Geophys. Res. Lett.*, *25*(20), 3799–3802, doi:10.1029/1998GL900003.
- McCoy, J. E., R. P. Lin, R. E. McGuire, L. M. Chase, and K. A. Anderson (1975), Magnetotail electric fields observed from lunar orbit, *J. Geophys. Res.*, *80*(22), 3217–3224, doi:10.1029/JA080i022p03217.
- McFadden, J. P., et al. (2008), The THEMIS ESA plasma instrument and in-flight calibration, *Space Sci. Rev.*, *141*, 277–302.
- Mendillo, M., B. Flynn, and J. Baumgardner (1993), Imaging experiments to detect an extended sodium atmosphere on the Moon, *Adv. Space Res.*, *13*(10), 313–319.
- Potter, A. E., R. M. Killen, and T. H. Morgan (2000), Variation of lunar sodium during passage of the Moon through the Earth's magnetotail, *J. Geophys. Res.*, *105*(E6), 15,073–15,084.
- Reasoner, D. L., and W. J. Burke (1972), Characteristics of the lunar photoelectron layer in the geomagnetic tail, *J. Geophys. Res.*, *77*(34), 6671–6687.
- Saito, Y., et al. (2010), In-flight performance and initial results of Plasma Energy Angle and Composition Experiment (PACE) on SELENE (Kaguya), *Space Sci. Rev.*, *154*, 265–303.
- Sarantos, M., R. E. Hartle, R. M. Killen, Y. Saito, J. A. Slavin, and A. Gloer (2012), Flux estimates of ions from the lunar exosphere, *Geophys. Res. Lett.*, *39*, L13101, doi:10.1029/2012GL052001.
- Smith, S. M., J. K. Wilson, J. Baumgardner, and M. Mendillo (1999), Discovery of the distant lunar sodium tail and its enhancement following the Leonid meteor shower of 1998, *Geophys. Res. Lett.*, *26*(12), 1649–1652, doi:10.1029/1999GL900314.
- Stern, S. A. (1999), The lunar atmosphere: History, status, current problems, and context, *Rev. Geophys.*, *37*(4), 453–491, doi:10.1029/1999RG900005.
- Tanaka, T., et al. (2009), First in situ observation of the Moon-originating ions in the Earth's magnetosphere by MAP-PACE on SELENE (KAGUYA), *Geophys. Res. Lett.*, *36*, L22106, doi:10.1029/2009GL040682.
- Troshichev, O., S. Kokubun, Y. Kamide, A. Nishida, T. Mukai, and T. Yamamoto (1999), Convection in the distant magnetotail under extremely quiet and weakly disturbed conditions, *J. Geophys. Res.*, *104*(A5), 10,249–10,263, doi:10.1029/1998JA900141.
- Wilson, J. K., M. Mendillo, and H. E. Spence (2006), Magnetospheric influence on the Moon's exosphere, *J. Geophys. Res.*, *111*, A07207, doi:10.1029/2005JA011364.
- Yokota, S., et al. (2009), First direct detection of ions originating from the Moon by MAP-PACE IMA onboard SELENE (KAGUYA), *Geophys. Res. Lett.*, *36*, L11201, doi:10.1029/2009GL038185.